

Impact of mass transfer coefficient correlations on prediction of reactive distillation column behaviour

Z. Švandová, J. Markoš*, Ľ. Jelemenský

Institute of Chemical and Environmental Engineering, Faculty of Chemical and Food Technology, Slovak University of Technology, Radlinského 9, 812 37 Bratislava, Slovak Republic

Received 20 June 2007; received in revised form 25 October 2007; accepted 26 October 2007

Abstract

A significant part of the safety analysis of a reactive distillation column is the identification of multiple steady states and their stability. A reliable prediction of multiple steady states in a reactive distillation column is influenced by the selection of an adequate mathematical model.

For modelling reactive distillation columns, equilibrium (EQ) and nonequilibrium (NEQ) models are available in the literature. The accuracy of the nonequilibrium stage model seems to be limited mainly by the accuracy of the correlations used to estimate the mass transfer coefficient and interfacial area.

The binary mass transfer coefficients obtained from empirical correlations are functions of the tray design and layout, or of the packing type and size, as well as of the operational conditions and physical properties of the vapour and liquid mixtures.

In this contribution, the nonequilibrium model was used for the simulation of a reactive distillation column. For prediction of the binary mass transfer coefficient for a sieve tray, four correlations were chosen to show their impact on the prediction of the reactive distillation column behaviour. As a model reactive distillation system, the synthesis of methyl tertiary-butyl ether (MTBE) was chosen. The steady-state analysis and the dynamic simulation of the model system were done. Qualitative differences between the steady states were predicted using the chosen correlations.

© 2007 Elsevier B.V. All rights reserved.

Keywords: Reactive distillation; Mass transfer coefficient; Nonequilibrium model; Multiple steady states; Sensitivity to model parameters prediction

1. Introduction

European direction 96/82/EC (and also Slovak Act 261/2002) on control of major industrial accidents (so called Seveso II) requires a detailed safety analysis not only for existing industrial units, but also for units (technologies, equipments) which are designed. As a useful tool for such an analysis is mathematical model of the equipment, linked with some methodology used for safety analysis like HAZOP or others. There are a lot of papers in literature, dealing with such topics, some of them have been published by our group [1–5]. Major parts of these works are dealing with automatic generation of a safety analysis questionnaire (what will happen in equipment if something is happening, e.g. increase of feed concentration, feed flow, etc.) and evaluation of the answers generated by the mathematical model. But, usually these models are very simple

(related to reactors: pseudo-homogeneous models, ideal flow, etc.).

To make a design and safety analysis of a new equipment during its projection using its mathematical model, the model parameters should be estimated from an independent experiment (usually kinetic parameters) or “*a priori*” from a literature survey—prediction of mass transfer and heat transfer coefficients using empirical or semi-empirical correlations.

A significant part of the safety analysis of a reactive distillation column (as well as of various types of chemical reactors (see Ref. [6])) is the identification of multiple steady states and their stability. Taylor and Krishna [7] reported that the combination of distillative separation with a chemical reaction leads to a complex interaction between the vapour–liquid equilibrium, vapour–liquid mass transfer, intra-catalyst diffusion (for heterogeneously catalysed processes) and chemical kinetics. According to their analysis, the nonequilibrium rate based model (applying the Maxwell-Stephan theory with the two film theory to describe mass and heat transfer thorough the vapour–liquid interphase) provides the best results in describing

* Corresponding author.

E-mail address: jozef.markos@stuba.sk (J. Markoš).

Nomenclature

a	total interfacial area (m^2)
c	molar concentration (mol m^{-3})
E^{MV}	Murphree tray efficiency
F	feed stream (mol s^{-1})
J	molar diffusion flux relative to the molar average velocity ($\text{mol m}^{-2} \text{s}^{-1}$)
$[k]$	matrix of multicomponent low-flux mass transfer coefficients (m s^{-1})
N_{I}	number of components
N_{s}	number of stages
\mathcal{N}	mass transfer rate (mol s^{-1})
r	formation rate (mol s^{-1})
$[R]$	matrix of mass transfer resistances (s m^{-1})
t	time (s)
T	temperature (K)
x	mole fraction in the liquid phase
X_{IB}	conversion of isobutene
y	mole fraction in the vapour phase
z^P	mole fraction for phase P

Greek letters

$[G]$	matrix of thermodynamic factors
κ^P	binary low-flux mass transfer coefficient for phase P (m s^{-1})

Superscripts

I	referring to the interface
L	referring to the liquid phase
V	referring to the vapour phase

Subscripts

i, k	component index
j	stage index
t	referring to the total mixture

both the steady state and the dynamic behaviour of a reactive distillation column. Mohl et al. [8], Thiel et al. [9], Jacobs and Krishna [10], Higler et al. [11] reported that RD columns can exhibit multiple steady states, which has been verified in experimental laboratory and pilot plant units. Very characteristic types of multiple steady states are isolated branches of solutions, also called isolas. The first example of an isola in a reactive distillation column was reported by Chen et al. [12]. In their case studies, isolated solution branches were found at several values of the Damköhler number. A reliable prediction of multiple steady states in a reactive distillation column (as well as in chemical reactors) is influenced by the selection of an adequate mathematical model. For modelling reactive distillation columns, the equilibrium (EQ) and nonequilibrium (NEQ) models are available in literature [7,13,14]. Existence of MSS can result in dangerous situations, although more frequently in technological problems. As was shown in our previous papers, the MSS can be predicted by both, EQ and NEQ, models for RD

in a CSTR with condenser [15,16] and for an RD column [17], however, the bifurcation diagrams obtained by these two model approaches have different shape (region of the parameter values in which these multiplicities occur).

Baur et al. [18] compared the EQ and the NEQ models for the methyl tertiary-butyl ether (MTBE) production in a reactive distillation column to find that while multiple steady states are exhibited by both modelling approaches, the “window” in which these multiplicities occur is significantly reduced in the NEQ model. A similar result was published by Švandová et al. [5,16] for the MTBE production in a CSTR with a total condenser, with the conclusion that the phenomena of multiple steady states are found in both models. However, the localisation of multiple steady-state zones in the two parameter plane predicted by the EQ and NEQ models can be different. The multiple steady-state zones predicted by the NEQ model are smaller compared to the zones predicted by the EQ model. Higler et al. [11] compared the EQ and NEQ model and presented a sensitivity analysis for the NEQ model in which the mass transfer coefficient was 90 and 110% of the base case (they used the correlation of Onda (1968) for a packed section of the column and the AIChE method for a sieve tray, see Table 1) Their conclusions are that the NEQ model shows significant quantitative differences from the EQ model. Furthermore, counter-intuitive effects were observed for the NEQ low-conversion “branch”. For example, increasing the mass transfer coefficient decreases the conversion of the low-conversion branch.

In this contribution, the nonequilibrium model was used for the simulation of a reactive distillation column. The Maxwell-Stefan approach was used to describe the interphase transport, with four different correlations used for the binary (Maxwell-Stefan) mass transfer coefficients prediction. To describe the V–L mass (and heat) transfer, the knowledge of binary mass transfer coefficients is required. Taylor and Krishna [14], Kooijman and Taylor [19] suggested, in their books, some correlations for their prediction, as it is reported in Table 1 of the manuscript. The user can choose any of the proposed correlations, depending on his experience and concept of the final column hardware realisation. It can be seen from Table 1 that practically all these correlations are 10–20 years old and were proposed on the basis of experimental data obtained from columns with specific hardware (tray construction, type of packing, catalyst deposit, etc.) used at that time. In the present time, a new sophisticated hardware is used (both for packing and tray construction, see web page of Sulzer, Montz or Koch Glitch companies [20,21], papers of professor Górák’s group [22–27], etc. Unfortunately, correlations for binary mass transfer coefficients have not been published yet.

The aim of the presented paper is to show the impact of these parameters on the prediction of the reactive distillation column behaviour. The steady-state analysis and the dynamic simulation of the model system were done. Qualitative differences between the steady states were predicted using the four chosen correlations.

What we tried to show in our paper, and in our opinion we did, is the fact, that an industrial multiphase chemical reactor is a very complex device, and its description by some “universal model”,

Table 1
Available mass transfer coefficient correlations per internal type suggested by Ref. [19]

Bubble-Cap tray	Sieve tray	Valve tray	Dumped packing	Structured packing
AICHE (1958) Hughmark (1971)	AICHE (1958) Chan-Fair (1984) Zuiderweg (1982) Chen-Chuang (1993) Harris (1965) Bubble-Jet	AICHE (1958)	Onda-Takeuchi-Okumoto (1968) Bravo-Fair (1982) Billert-Schultes (1992) –	Bravo-Rocha-Fair (1985) Bravo-Rocha-Fair (1992) Billet-Schultes (1992) –

or by a model taking into account all particular processes in the multiphase reactor, is still impossible. Even if the rigorous model is used, there is still lack of accurate estimations of all parameters of the model. Doing the projection (design) of a new RDC, it is clear that its hardware solution depends strongly on the available market. However, for the newest available hardware, there are still no correlations for model parameters prediction in the literature. The use of incorrect literature correlations can lead to errors in the column behaviour prediction.

2. Theoretical

The NEQ model for reactive distillation follows the philosophy of rate based models for conventional distillation [28], including the chemical reaction terms.

The key feature of the nonequilibrium model is that the conservation equations are written for each phase independently and solved together with the transport equations that describe the mass and energy transfer in multicomponent mixtures. The equilibrium is assumed to exist only at the phase interface. The description of the interphase mass transfer in either fluid phase is based on the Maxwell-Stefan theory for calculation of the interphase heat and mass transfer rates [14].

At the V–L interface there is a continuity of the molar fluxes \mathcal{N}_i^V and \mathcal{N}_i^L :

$$\mathcal{N}_i^V = \mathcal{N}_i^L \quad (1)$$

To evaluate the molar fluxes, which include both diffusive and convective contributions, the composition of the phases leaving stage j was used as the bulk phase composition. The bulk phases are assumed to be completely mixed and the mass transfer from the vapour phase to the liquid phase leads to a positive flux. The column matrices of mass transfer rates in each phase are given by equations:

$$\left(\mathcal{N}_j^V\right) = c_{t,j}^V \left[k_j^V\right] a_j \left(y_j - y_j^I\right) + \mathcal{N}_{t,j}^V(y_j) \quad (2)$$

$$\left(\mathcal{N}_j^L\right) = c_{t,j}^L \left[k_j^L\right] a_j \left(x_j^I - x_j\right) + \mathcal{N}_{t,j}^L(x_j) \quad (3)$$

where a_j is the net interfacial area for stage j , (x_j) and (y_j) represent the column vectors of mole fractions of the species in the bulk liquid and bulk vapour phase, respectively, (x_j^I) and (y_j^I) represent the column vectors of mole fractions of the species on the liquid–vapour interface, c_t^L and c_t^V are the total mixture molar concentrations for the liquid and vapour phase, respectively, and \mathcal{N}_t is the total mass transfer rate. Note that there are only $(N_I - 1) \times (N_I - 1)$ elements in the $[k]$ matrices and,

therefore there are only $(N_I - 1)$ equations for the mass transfer rate.

The matrices of multicomponent mass transfer coefficients $[k^V]$ and $[k^L]$ were calculated from:

$$[k^V] = [R^V]^{-1} \quad (4)$$

$$[k^L] = [R^L]^{-1} [\Gamma] \quad (5)$$

where $[\Gamma]$ is the matrix of thermodynamic correction factors portraying the non-ideal behaviour and $[R]$ is the matrix of mass transfer resistances calculated from the following formulae:

$$R_{i,i}^P = \frac{z_i^P}{\kappa_{i,N_I}^P} + \sum_{\substack{k=1 \\ k \neq i}}^{N_I} \frac{z_k^P}{\kappa_{i,k}^P} \quad (6)$$

$$R_{i,j(i \neq j)}^P = -z_i^P \left(\frac{1}{\kappa_{i,j}^P} - \frac{1}{\kappa_{i,N_I}^P} \right) \quad (7)$$

where z^P is the mole fraction for phase P and $\kappa_{i,j}^P$ is the low-flux mass transfer coefficient for the binary i – j pair for phase P . The low-flux mass transfer coefficients $\kappa_{i,j}^P$ were estimated using empirical correlations with the Maxwell-Stefan diffusivity of the appropriate i – j pair replacing the binary Fick's diffusivity (for details see Ref. [14]).

Table 1 provides a summary of available correlations for trays and packings suggested by Ref. [19]. A summary of specific equations used to calculate the binary mass transfer coefficient is given for example by Taylor and Krishna [14] and Kooijman and Taylor [19].

The binary mass transfer coefficients obtained from these correlations are functions of the tray design and layout, or of the packing type and size, as well as of the operational parameters and physical properties including the binary pair Maxwell-Stefan diffusion coefficients. The accuracy of the nonequilibrium stage model seems to be limited mainly by the accuracy of the correlations used to estimate the mass transfer coefficient–interfacial area product [29].

To compare the reactive distillation column behaviour predicted by different correlations for mass transfer coefficients, the four correlations summarised in Table 2 were chosen.

For purposes of estimation of the diffusion coefficients in gas mixtures and in dilute liquid mixtures, the empirical correlations of Fuller-Schettler-Giddings (1966) and Wilke-Chang (1955), respectively, were used (for details see Refs. [14,30,31]). The Maxwell-Stefan diffusion coefficient is defined for each binary pair in the multicomponent liquid mixture using the

Table 2

Mass transfer coefficient correlations chosen for the investigation in this contribution

Model number	Mass transfer coefficient correlation	Specific equations are available in references
1	AICHE (1958)	[14,19,38]
2	Chan-Fair (1984)	[14,19,39]
3	Chen-Chuang (1993)	[19,40]
4	Zuiderweg (1982)	[14,19,41]

diffusion coefficients in dilute liquid. The mixing rule used is from Wesselingh and Krishna [32]. For the calculation of vapour and liquid phase heat transfer coefficients the Chilton-Colburn analogy between mass and heat transfers and the penetration model were used, respectively (for details see Ref. [19]).

3. Model system: production of MTBE in reactive distillation column

Primary reaction in MTBE production is the etherification of isobutene (IB) with methanol (MeOH) to form MTBE in the presence of a strong acid catalyst. The reaction is usually carried out in the presence of inert components. These inert components come from the upstream processing where isobutene is produced. In our case study, 1-butene (1B) is used as an inert. The reaction kinetic expression and parameters were taken from Rehfinger and Hoffmann [33]. Possible side-reactions were ignored. Reaction rates were calculated assuming a pseudo-homogeneous model.

For the calculation of mixed physicochemical properties, an internal software library was employed. Physicochemical properties of all pure components were taken from the HYSYS 2.1 database and from Ref. [30]. The vapour–liquid equilibrium was calculated using the UNIQUAC model with the binary interaction parameters reported by Rehfinger and Hoffmann [33] (all binary interactions between MeOH, IB, MTBE) and HYSYS

Table 3

Tray specifications

Type of tray	Sieve
Column diameter	6 m
Total tray area	28.27 m ²
Number of liquid flow passes	5
Tray spacing	0.61 m
Liquid flow path length	0.97 m
Fractional active area	0.76
Fractional hole area	0.1
Fractional downcomer area	0.12
Hole diameter	4.5 mm
Weir height	50 mm
Total weir length	22 m

2.1 (all binary interactions between 1-butene and the other components). The gas phase was supposed to be ideal.

The column configuration chosen for the simulations was described by Jacobs and Krishna [10]. The column consisted of a total condenser, 15 sieve trays (2 rectifying stages, 8 reactive stages and 5 stripping stages), and a partial reboiler. On each of the eight reactive stages in the reactive zone, 1000 kg of the catalyst were charged in the form of “envelopes” placed along the flow path length. The details of such a construction are available in the patent [34].

The column pressure was 1110 kPa and the column had two feed streams: methanol feed and mixed butenes feed, both fed to stage 10. At a standard operating point, the molar flow rates of pure methanol (F^L) and the mixture of butenes (F^V) were 775.8 and 1900 kmol h⁻¹, respectively. The mixed butenes feed consisted of 35.58% isobutene and 64.42% 1-butene. The reflux ratio was set to 7 and the bottom flow rate to 675 kmol h⁻¹. The detailed specifications of the sieve trays are given in Table 3.

4. Results and discussion

The steady-state behaviour of the reactive distillation column described by the NEQ model was investigated using the continuation algorithm CONT taken from Ref. [35]. The four

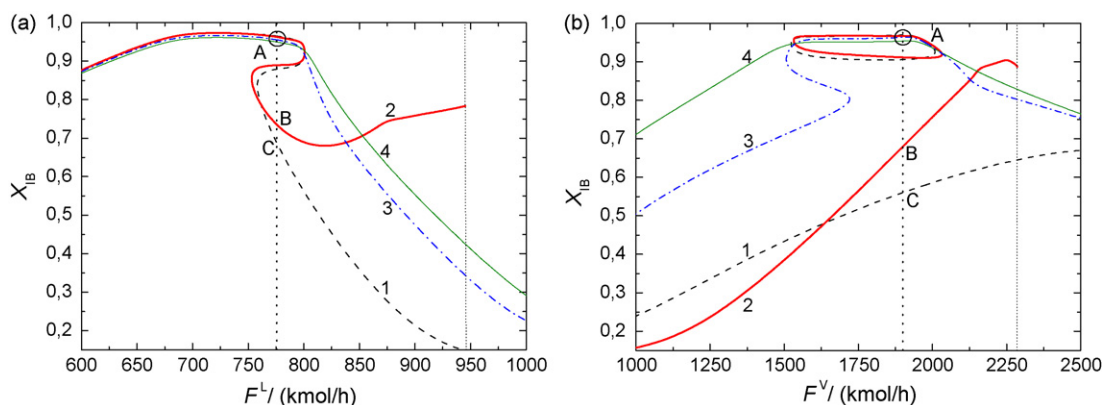


Fig. 1. (a) Conversion of isobutene vs. methanol feed flow rate solution diagrams. (b) Conversion of isobutene vs. butenes feed flow rate solution diagrams (dashed line—Model 1, thick solid line—Model 2, dash-dotted line—Model 3, thin solid line—Model 4, vertical dotted line—operating feed flow rate, vertical short dotted line—Model 2 out of the validity range).

Table 4

Summary of isobutene conversion and MTBE purity in reboiler for stable steady states predicted by all used models

	Upper stable steady state		Lower stable steady state	
	Conversion of isobutene	Purity of MTBE in reboiler	Conversion of isobutene	Purity of MTBE in reboiler
Model 1	0.9695	0.9698	0.5603	0.5281
Model 2	0.9671	0.9668	0.6798	0.6183
Model 3	0.9639	0.9644	–	–
Model 4	0.9540	0.9539	–	–

correlations of the mass transfer coefficient for a sieve tray (list in Table 2) were used to calculate the binary mass transfer coefficients.

In the solution diagrams (Fig. 1a and b) either the methanol feed flow rate (with constant butenes feed flow rate set to the value 1900 kmol h^{-1}) or the butenes feed flow rate (with constant methanol feed flow rate set to the value $775.8 \text{ kmol h}^{-1}$) were the continuation parameters. The conversion of isobutene (X_{IB}) was examined. The isobutene conversion (X_{IB}) was in our case study defined as the difference between the ‘fresh isobutene molar feed flow rate into the reactive distillation column’ and the ‘molar flow rate of isobutene in the output streams of the reactive distillation column’ divided by the ‘fresh isobutene molar feed flow rate into the reactive distillation column’.

The solution diagrams (Fig. 1a), where the methanol feed flow rate was used as the continuation parameter, indicate that multiple steady states are predicted by Models 1 and 2. Using parameters calculated by Models 3 and 4, no multiplicity occurred in the whole range of the investigated parameter. When the isobutene feed flow rate was used as the continuation parameter, multiple steady states existed for three of the four investigated methods (Fig. 1b). Only when using parameters calculated by Model 4, no multiplicity occurred in the whole range of the investigated parameter. However, a very interesting result is that Models 1 and 2 predict continuous curves of the isobutene conversion with isolas located above these curves. Model 3 predicts a typical ‘S’ profile of the isobutene conversion and, at the same time, the “window” in which these multiplicities occur is significantly reduced.

In general, the AICHE method (Model 1) and the Chan-Fair method (Model 2) behave in essentially the same way, except for the strong dependence on the fraction of flooding in the Chan-Fair method (Model 2). The critics of the Chan-Fair (Model 2) correlation mention that the quadratic dependence on the fractional approach to flooding limits this correlation to the range of fractions of flooding where the quadratic term is positive (the fraction of flooding must lie between 0 and 1.2) [36]. We have encountered situations of the Chan-Fair (Model 2) correlations providing negative mass transfer coefficient because the fraction of flooding was outside this range. It is clear that negative mass transfer coefficients are physically meaningless, at the same time the program that implements our nonequilibrium model stopped converging to the solution. This situation is represented in the solution diagrams (Fig. 1) by a short vertical dotted line ($F^L \approx 948 \text{ kmol h}^{-1}$ in Fig. 1a. and $F^V \approx 2280 \text{ kmol h}^{-1}$ in Fig. 1b).

From the solution diagrams (Fig. 1a and b) follows that for the given operating feed flow rate of methanol ($F^L = 775.8 \text{ kmol h}^{-1}$, see dotted line in Fig. 1a) and operating feed flow rate of butenes ($F^V = 1900 \text{ kmol h}^{-1}$, see dotted line in Fig. 1b) predict the Models 1 and 2 three steady states (two stable, one unstable), however, Models 3 and 4 predict only one steady state. The steady states obtained by Models 3 and 4 are nearly equal to the upper steady states given by Models 1 and 2. Table 4 contains a summary of the conversion of isobutene and the purity of MTBE in the reboiler for the stable steady states predicted by all four models. From this table is clear that the conversion of isobutene and the purity of MTBE in the upper steady states are nearly identical for all used models. However, the conversion of isobutene and the purity of MTBE are relatively different for Models 1 and 2 in the lower steady state.

The presence of multiple steady states strongly influences the reactive distillation column behaviour during its start-up as well as during any disturbances of the input parameters. For illustration, disturbances of the butenes feed flow rate were studied (Fig. 2) starting from the operational steady states characterised by high conversion of isobutene. At 1 h, a very fast increase of the butenes feed flow rate, over 2100 kmol h^{-1} , was simulated. The original flow rate of butenes was reached 10 h later. The duration of the disturbance was so long to show that for all investigated methods, a new steady state corresponding to butenes feed flow rate 2100 kmol h^{-1} was reached. After returning the butenes flow rate to the operational value, the system described with the NEQ model using Models 1 and 2 was stabilised in the lower

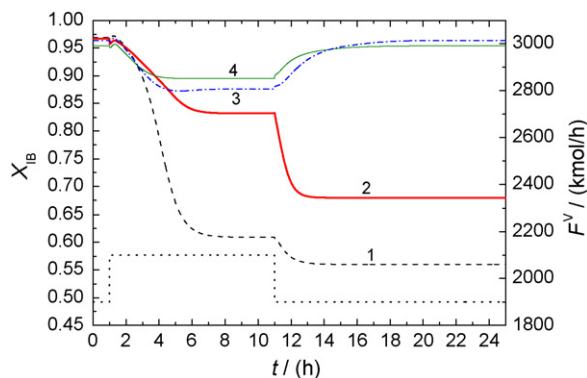


Fig. 2. Conversion of isobutene changes after step change of the butenes feed flow rate from the value of $1900\text{--}2100 \text{ kmol h}^{-1}$ and back (dashed line—Model 1, thick solid line—Model 2, dash-dotted line—Model 3, thin solid line—Model 4, dotted line—butenes feed flow rate).

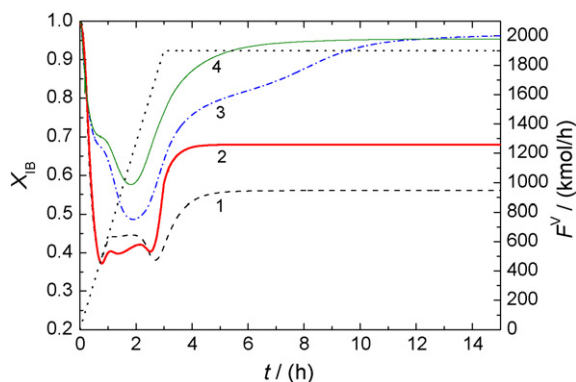


Fig. 3. Columns start-up considering a gradual increase of the butenes feed flow rate (dashed line—Model 1, thick solid line—Model 2, dash-dotted line—Model 3, thin solid line—Model 4, dotted line—butenes feed flow rate).

stable steady state. But providing the NEQ model with Models 3 or 4, the system worked again in the original steady state (see Fig. 2). From Fig. 2 follows that for situations predicted by Models 1 and 2, the restart of the RD column is needed to switch the conversion to higher steady states.

However, the presence of multiple steady states reduces the operability and controllability of the reactive distillation column during its start-up. This is validated in Fig. 3 which represents the column start-up considering a gradual increase of the butenes feed flow rate. Before the start-up procedure, the column was filled with pure methanol. Applying this start-up procedure, after reaching the operational feed flow rate of butenes, Models 1 and 2 predicted column stabilisation in the steady state characterised by low conversion of isobutene. Models 3 and 4 predict only one possible steady state for the operating feed flow rate of butenes (see Fig. 1b), hence, after the start-up procedure, this steady state is reached (Fig. 3).

Figs. 4 and 5 show the MTBE formation rates and temperature profiles in the liquid phase, for the upper (full lines) and lower (dotted lines) stable steady states, respectively, as predicted by all investigated models.

In the low-conversion steady states (dotted lines in Fig. 4) predicted by Models 1 and 2, MTBE was formed in the upper part of

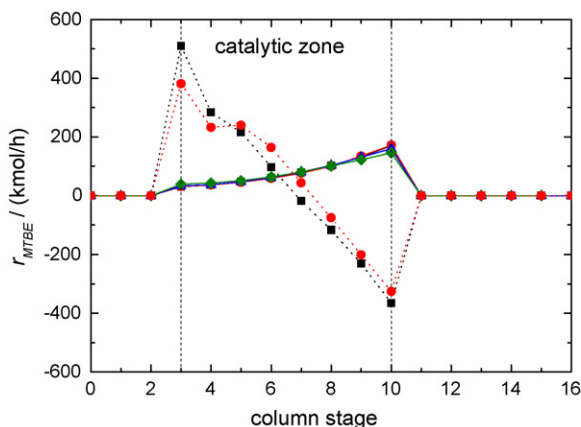


Fig. 4. MTBE formation rates (■ Model 1, ● Model 2, ▲ Model 3, ◆ Model 4, dotted lines—lower stable steady states, full lines—upper stable steady states).

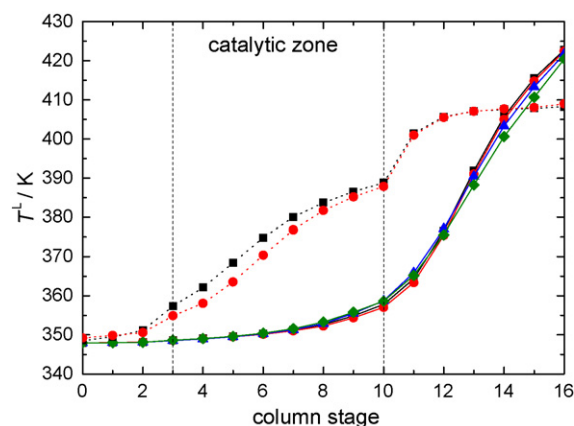


Fig. 5. Temperature profiles in liquid phase (■ Model 1, ● Model 2, ▲ Model 3, ◆ Model 4, dotted lines—lower stable steady states, full lines—upper stable steady states).

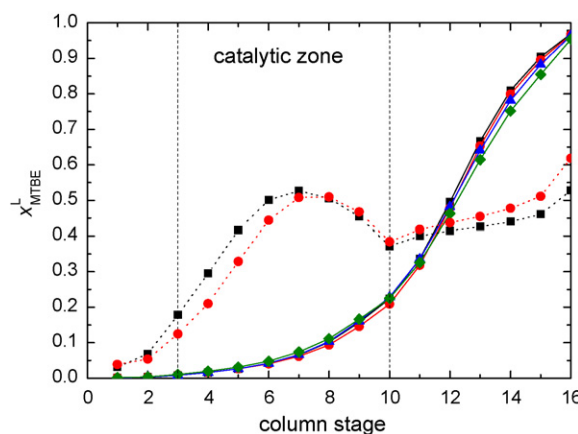


Fig. 6. Molar fraction of MTBE in bulk liquid phase (■ Model 1, ● Model 2, ▲ Model 3, ◆ Model 4, dotted lines—lower stable steady states, full lines—upper stable steady states).

the reaction zone. In the lower part of the reaction zone, the reaction was reversed, MTBE decomposed. In the high-conversion steady states (full lines in Fig. 4), MTBE was formed in the entire reaction zone and by contrast with the low-conversion

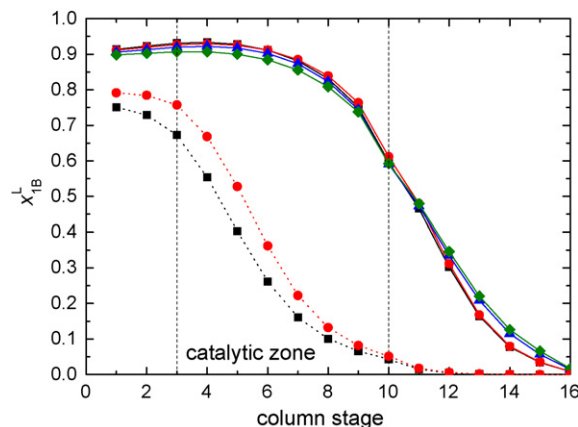


Fig. 7. Molar fraction of 1-butene in bulk liquid phase (■ Model 1, ● Model 2, ▲ Model 3, ◆ Model 4, dotted lines—lower stable steady states, full lines—upper stable steady states).

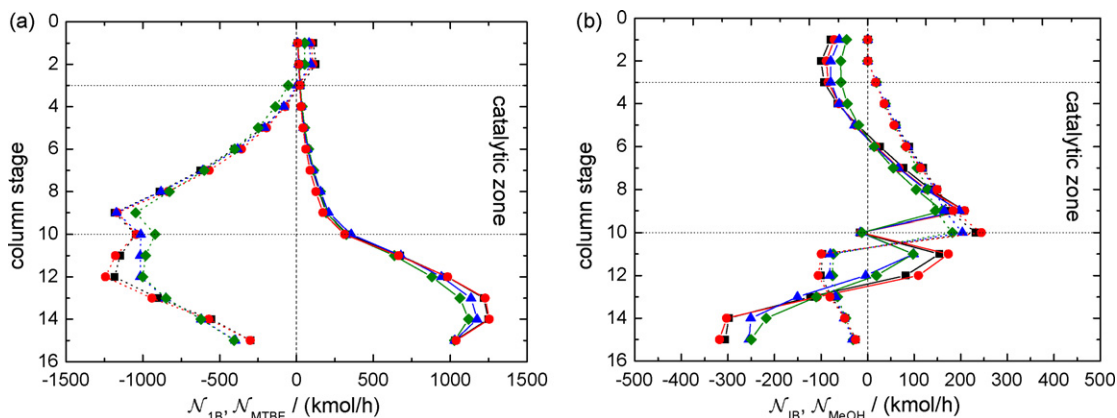


Fig. 8. (a) MTBE (full lines) and 1-butene (dotted lines) mass transfer rates in upper steady state. (b) Methanol (full lines) and isobutene (dotted lines) mass transfer rates in upper steady state ((■) Model 1, (●) Model 2, (▲) Model 3, (◆) Model 4).

steady states, its formation rates were the highest in the lower part of the reaction zone.

The temperature profiles in the reactive zone, shown in Fig. 5, are connected with the composition. In the low-conversion case, there was a lot of MTBE on the reactive trays (see Fig. 6), there is, however, a smaller amount of the inert compared to the higher conversion case (see Fig. 7). Consequently, in the higher conversion case, lower temperature on the reactive trays (see Fig. 5) is connected with a great amount of the inert which dilutes the mixture. In the lower conversion case, higher temperature on the reactive trays is connected with a great amount of MBTE and a smaller amount of the inert, which leads to the decomposition of MTBE in the lower part of the reactive zone (see Fig. 4).

The presence of a sufficient amount of an inert component plays a key role in the occurrence of multiple steady states in the MTBE process as explained by Hauan et al. [37].

Figs. 8a and b and 9a and b show the mass transfer rates, for the upper and lower stable steady state, respectively, as predicted by all investigated methods. Transfer from the vapour to the liquid phase leading to a positive flux was considered.

Fig. 8a shows the 1-butene (dotted lines) and MTBE (full lines) mass transfer rates in the upper stable steady state for all investigated methods. From this picture is clear that massive evaporation of 1-butene occurred in the lower part of the column, because a large amount of 1-butene was present in the liquid phase (see Fig. 7). At the same time, MTBE concentrated in the liquid phase, in the lowest part of the column under the reactive zone, preventing MTBE from decomposition. Another good trend in the upper steady-state case is that the isobutene (dotted lines in Fig. 8b) condensed to the liquid phase in the reactive section, to allow reaction with methanol to form MTBE.

Fig. 9a shows the 1-butene (dotted lines) and MTBE (full lines) mass transfer rates in the lower stable steady states predicted by Models 1 and 2. From Fig. 9a results that massive evaporation of 1-butene from the liquid phase is dominantly present in the upper part of the column (dotted line in Fig. 9a). At the same time, isobutene (dotted line in Fig. 9b) condensed to the liquid phase only in the upper part of the reactive section, where MTBE is consequently produced. In the lower part of the reactive section, MTBE is decomposed, because of an insufficient amount of 1-butene for dilution.

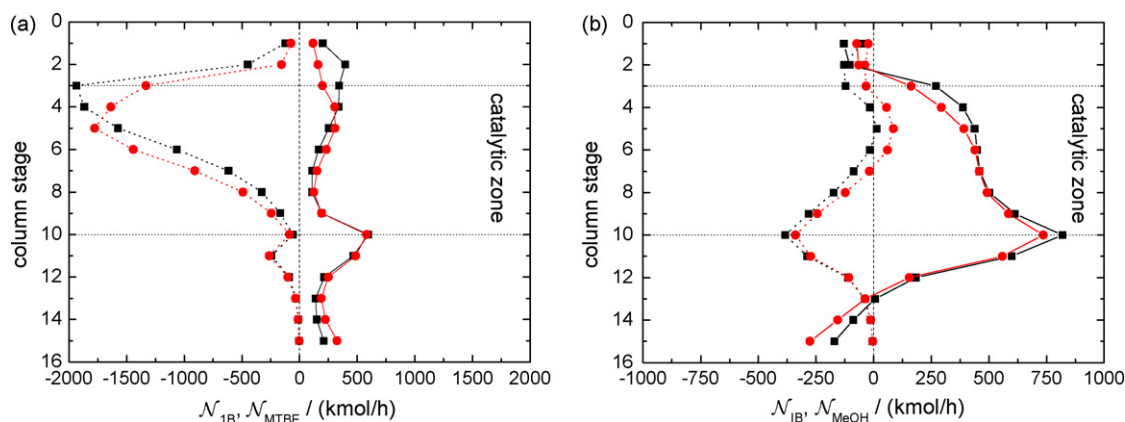


Fig. 9. (a) MTBE (full lines) and 1-butene (dotted lines) mass transfer rates in lower steady state. (b) Methanol (full lines) and isobutene (dotted lines) mass transfer rates in lower steady state ((■) Model 1, (●) Model 2, (▲) Model 3, (◆) Model 4).

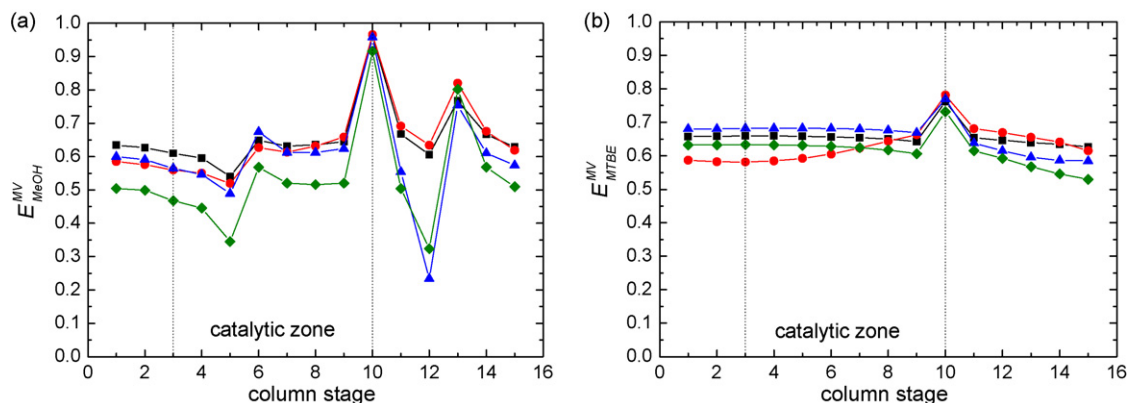


Fig. 10. (a) Murphree tray efficiency in upper steady state for methanol. (b) Murphree tray efficiency in upper steady state for MTBE (■) Model 1, (●) Model 2, (▲) Model 3, (◆) Model 4).

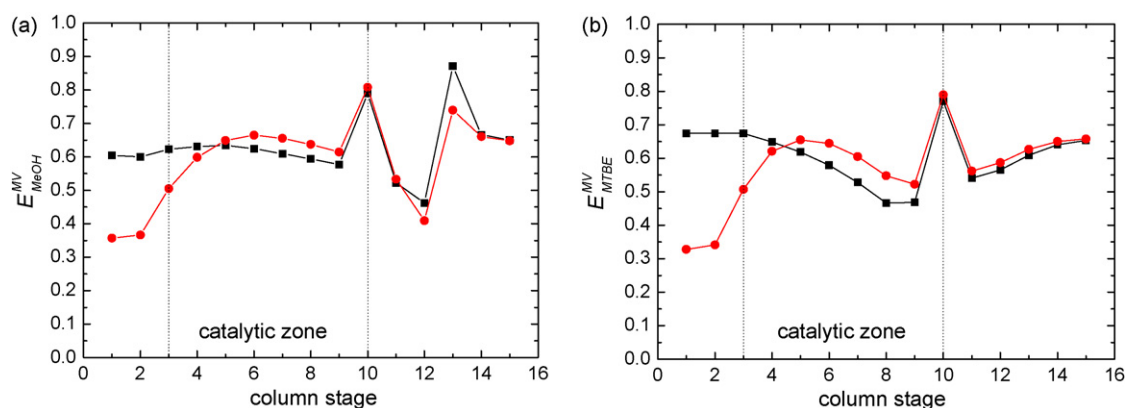


Fig. 11. (a) Murphree tray efficiency in lower steady state for methanol. (b) Murphree tray efficiency in lower steady state for MTBE (■) Model 1, (●) Model 2).

From Figs. 1–8 follows that all used models predict the high-conversion steady state in good agreement with each other. This tendency can be observed also in Fig. 10a and b which shows the Murphree tray efficiency for methanol and MTBE in the upper (high conversion) steady state, respectively. These pictures indicate, that Model 4 tends to predict a lower Murphree tray efficiency compared to other methods, however, this does not markedly affect the conversion of isobutene and the purity of MTBE in the reboiler.

For the given operational conditions, the low-conversion steady state was predicted only by Models 1 and 2. The difference between the low-conversion steady states predicted by Models 1 and 2 is more relevant. For the lower steady state, Model 1 predicted a slightly higher temperature in the reaction zone than Model 2 (dotted lines in Fig. 5) and simultaneously, Model 1 predicted a higher MTBE formation rate in the upper part of the reaction zone and consequently a higher rate of decomposition in the lower part of the reaction zone (dotted lines in Fig. 4). However, Model 2 predicted, for the low-conversion steady state, higher conversion than Model 1.

Fig. 11a and b shows the Murphree tray efficiency for methanol and MTBE, respectively, in the low-conversion steady state. These pictures show that in the lower part of the reactive zone (stages 5–10) Model 2 predicts higher Murphree tray efficiency, which hinders the decomposition of MBTE. Model 2

predicts a radical decrease of the Murphree tray efficiency in the upper part of the column (stages 1–4). This behaviour predicted by Model 2 is caused by the quadratic dependence on the fractional approach to flooding, as, in this part of the column, is the fraction of flooding close to unity, thus close to flooding.

5. Conclusions

The sensitivity of simulation results of a reactive distillation column, with model system of the MTBE synthesis, using a complex NEQ mathematical model for the mass transfer parameters prediction, is presented in the paper.

A reliable prediction of the reactive distillation column behaviour is influenced by the complexity of the mathematical model which is used for its description. For reactive distillation column modelling, equilibrium and nonequilibrium models are available in the literature. Moreover, the quality of a nonequilibrium model differs with the reference to the description of the vapour–liquid equilibria, reaction equilibria and kinetics (homogenous, heterogeneous reaction, pseudo-homogenous approach), mass transfer (effective diffusivity method, Maxwell-Stefan approach) and hydrodynamics (completely mixed vapour and liquid, plug-flow vapour, eddy diffusion model for the liquid phase, etc.). It is obvious that different model approaches lead

more or less to different predictions of the reactive distillation column behaviour.

In the presented paper, the Maxwell-Stefan approach was used to describe interphase transport with four different correlations used for the binary (Maxwell-Stefan) mass transfer coefficient estimation. As it was shown, different correlations used for the prediction of these parameters lead to significant differences in the prediction of the reactive distillation column behaviour.

At the present time, considerable progress has been made regarding the reactive distillation column hardware aspects (tray design and layout, packing type and size). If mathematical modelling should be a useful tool for optimisation, design, scale up and safety analysis of a reactive distillation column, the correlations applied in model parameter predictions have to be carefully chosen and employed for concrete column hardware. A problem could arise if, for a novel column hardware, such correlations are still not available in the literature, e.g. the correlation and model quality progress are not equivalent to the hardware progress of the reactive distillation column.

As is possible to see from Fig. 1a and b, for given operational conditions and “good” initial guess of calculated column variables (V and L concentrations and temperature profiles, etc.) NEQ model given by a system of non-linear algebraic equations converged practically to the same steady state with high conversion of isobutene (point A in Fig. 1) with all assumed correlations. If “wrong” initial guess is chosen, the NEQ model can provide different results according applied correlation: point A for Models 3 and 4 with high conversion of isobutene, point B for Model 2 and point C for Model 1. Therefore the analysis of multiple steady-states existence has to be done as the first step of safety analysis. If we assume the operational steady state of column given by point A, and we start the generate HAZOP deviation of operational parameters, by dynamic simulation we can obtain for each correlation different prediction of column behaviour, see Fig. 2. Also dynamic simulation of column start-up procedure from the same initial conditions (for NEQ model equations) results to the different steady state depending on chosen correlation, see Fig. 3.

Our point of view is that of an engineer who has to do a safety analysis of an RDC using the mathematical model of such a device. Collecting literature information, he can discover that there are a lot of papers dealing with mathematical modelling. As was mentioned above, Taylor and Krishna [7] cite over one hundred papers dealing with mathematical modelling of RD of different complexity. And there is the problem: which model is the best and how to obtain parameters for the chosen model. There are no general guidelines in the literature. Using correlations suggested by authorities, the engineer can get into troubles. If different models predict different MSS in an RDC for the same column configuration and the same operational conditions, they also predict different dynamic behaviour, and provide different answers on deviations generated by HAZOP. Consequently, it can lead to different definition of the operator’s strategy under normal and abnormal conditions and training of operational staff.

Acknowledgement

This work was supported by the Science and Technology Assistance Agency under the contract No. APVT-20-000804.

References

- [1] Z. Švandová, L. Jelemenský, J. Markoš, A. Molnár, Steady state analysis and dynamical simulation as a complement in the HAZOP study of chemical reactors, *Trans. IChemE, Part B: Process Saf. Environ. Prot.* 83 (B5) (2005) 463–471.
- [2] Z. Švandová, J. Markoš, L. Jelemenský, HAZOP analysis of CSTR with utilization of mathematical modeling, *Chem. Pap.* 59 (6b) (2005) 464–468.
- [3] J. Labovský, L. Jelemenský, J. Markoš, Safety analysis and risk identification for tubular reactor using the HAZOP methodology, *Chem. Pap.* 60 (6) (2006) 454–459.
- [4] J. Labovský, Z. Švandová, J. Markoš, L. Jelemenský, Model-based HAZOP study of a real MTBE plant, *J. Loss Prev. Proc.* 20 (3) (2007) 230–237.
- [5] J. Labovský, Z. Švandová, J. Markoš, L. Jelemenský, Mathematical model of a chemical reactor—useful tool for its safety analysis and design, *Chem. Eng. Sci.* 62 (2007) 4915–4919.
- [6] A. Molnár, J. Markoš, L. Jelemenský, Some considerations for safety analysis of chemical reactors, *Trans. IChemE, Part A: Chem. Eng. Res. Des.* 83 (A2) (2005) 167–176.
- [7] R. Taylor, R. Krishna, Modelling reactive distillation, *Chem. Eng. Sci.* 55 (22) (2000) 5183–5229.
- [8] K.-D. Mohl, A. Kienle, E.-D. Gilles, P. Rapmund, K. Sundmacher, U. Hoffmann, Steady-state multiplicities in reactive distillation columns for the production of fuel ethers MTBE and TAME: theoretical analysis and experimental verification, *Chem. Eng. Sci.* 54 (8) (1999) 1029–1043.
- [9] C. Thiel, P. Rapmund, K. Sundmacher, U. Hoffmann, K.D. Mohl, A. Kienle, E.D. Gilles, Intensified production of fuel ethers in reactive distillation columns—experimental validation of predicted multiple steady states, in: *Proceedings of the first European Congress on Chemical Engineering—ECCE-1*, vol. 2, Florence, 1997, pp. 1423–1426.
- [10] R. Jacobs, R. Krishna, Multiple solutions in reactive distillation for methyl tert-butyl ether synthesis, *Ind. Eng. Chem. Res.* 32 (8) (1993) 1706–1709.
- [11] A.P. Higler, R. Taylor, R. Krishna, Nonequilibrium modelling of reactive distillation: multiple steady states in MTBE synthesis, *Chem. Eng. Sci.* 54 (10) (1999) 1389–1395.
- [12] F. Chen, R.S. Huss, M.F. Doherty, M.F. Malone, Multiple steady states in reactive distillation: kinetic effects, *Comput. Chem. Eng.* 26 (1) (2002) 81–93.
- [13] C. Noeres, E.Y. Kenig, A. Górak, Modelling of reactive separation processes: reactive absorption and reactive distillation, *Chem. Eng. Process.* 42 (3) (2003) 157–178.
- [14] R. Taylor, R. Krishna, *Multicomponent Mass Transfer*, John Wiley & Sons, Inc., New York, 1993.
- [15] Z. Švandová, M. Kotora, J. Markoš, L. Jelemenský, Dynamic behaviour of a CSTR with reactive distillation, *Chem. Eng. J.* 119 (2006) 113–120.
- [16] Z. Švandová, J. Markoš, L. Jelemenský, Multiple steady states in a CSTR with total condenser: comparison of equilibrium and nonequilibrium models, *Chem. Pap.* 60 (6) (2006) 432–440.
- [17] Z. Švandová, J. Labovský, J. Markoš, L. Jelemenský, Impact of mathematical model selection on prediction of steady state and dynamic behaviour of a reactive distillation column, in: V. Plesu, P.S. Agachi (Eds.), *Computer Aided Chemical Engineering*, vol. 24, Elsevier, Amsterdam, 2007, pp. 1235–1240, ISBN 987-0-444-53157-5.
- [18] R. Baur, A.P. Higler, R. Taylor, R. Krishna, Comparison of equilibrium stage and nonequilibrium stage models for reactive distillation, *Chem. Eng. J.* 76 (1) (2000) 33–47.
- [19] H.A. Kooijman, R. Taylor, *The ChemSep Book*, Libri Books on Demand, Norderstedt, 2000.
- [20] <http://www.sulzerchemtech.com/desktopdefault.aspx>.
- [21] <http://www.koch-glitsch.com>.
- [22] A. Górak, L.U. Kreul, M. Skowronski, *Strukturierte Mehrzweckpakung*, Deutsches Patent 19,701,045 (1997).

- [23] A. Górák, Modelling reactive distillation, in: Proceedings of the 33rd International Conference of Slovak Society of Chemical Engineering, Tatranské Matliare, Slovakia, 2006, ISBN 80-227-2409-2 (Plenary lecture).
- [24] A. Kolodziej, A. Górák, M. Jaroszynski, Reactive distillation: a success story with obstacles, in: Proceedings of the 34th International Conference of Slovak Society of Chemical Engineering, Tatranské Matliare, Slovakia, 2007, ISBN 978-80-227-2640-5 (Plenary lecture).
- [25] INTINT project: Intelligent column internals for reactive separation, <http://www.cpi.umist.ac.uk/intint>.
- [26] C. Buchaly, P. Kreis, A. Górák, Hybrid separation processes—combination of reactive distillation with membrane separation, Chem. Eng. Process. 46 (9) (2007) 790–799.
- [27] M. Katora, C. Buchaly, P. Kreis, A. Górák, J. Markoš, Reactive distillation—experimental data for *n*-propyl propionate synthesis, Chem. Pap. 61(1) (2008), in press.
- [28] R. Krishnamurthy, R. Taylor, A nonequilibrium stage model of multicomponent separation processes. I—Model description and method of solution, AIChE J. 31 (3) (1985) 449–456.
- [29] R. Krishnamurthy, R. Taylor, A nonequilibrium stage model of multicomponent separation processes. II—Comparison with experiment, AIChE J. 31 (3) (1985) 456–465.
- [30] R.C. Reid, J.M. Prausnitz, T.K. Sherwood, The Properties of Gases and Liquids, third ed., McGraw-Hill, New York, 1977.
- [31] R.H. Perry, D.W. Green, J.O. Maloney, Perry's Chemical Engineers' Handbook, seventh ed., McGraw-Hill, New York, 1997.
- [32] J.A. Wesselingh, R. Krishna, Mass Transfer, Ellis Horwood, Chichester, England, 1990.
- [33] A. Rehfinger, U. Hoffmann, Kinetics of methyl tertiary butyl ether liquid phase synthesis catalyzed by ion exchange resin. I: Intrinsic rate expression in liquid phase activities, Chem. Eng. Sci. 45 (6) (1990) 1605–1617.
- [34] E.M. Jones Jr., Contact structure for use in catalytic distillation, US Patent 4,536,373 (1985).
- [35] M. Kubíček, Algorithm 502. Dependence of solution of nonlinear systems on a parameter [C5], ACM Trans. Math. Software 2 (1) (1976) 98–107.
- [36] H.A. Kooijman, R. Taylor, Modelling mass transfer in multicomponent distillation, Chem. Eng. J. 57 (2) (1995) 177–188.
- [37] S. Hauan, T. Hertzberg, K.M. Lien, Multiplicity in reactive distillation of MTBE, Comput. Chem. Eng. 21 (10) (1997) 1117–1124.
- [38] AIChE Bubble Tray Design Manual, AIChE, New York, 1958.
- [39] H. Chan, J.R. Fair, Prediction of point efficiencies on sieve trays. 1: Binary systems, Ind. Eng. Chem. Des. Dev. 23 (4) (1984) 814–819.
- [40] G.X. Chen, K.T. Chuang, Prediction of point efficiency for sieve trays in distillation, Ind. Eng. Chem. Res. 32 (1993) 701–708.
- [41] F.J. Zuiderweg, Sieve trays: a view on the state of the art, Chem. Eng. Sci. 37 (10) (1982) 1441–1464.